Petal-shaped MOF assembled with gold nanocage and urate oxidase used as artificial enzyme nanohybrid for tandem catalysis and dual-channel biosensing

Zejun Sun,[1] Yujiao Sun,[1] Meng Yang, Hui Jin,[*] and Rijun Gui [*]

College of Chemistry and Chemical Engineering, Intellectual Property Research Institute, Qingdao University, Shandong 266071, P.R. China.

[*] Corresponding authors

E-mail addresses: guirijun@qdu.edu.cn, jh8381@163.com.

[1] The co-first authors made equivalent contributions to this work.

2. Experimental section

2.1. Chemicals

In detail, $Zn(NO_3)_2 \cdot 6H_2O$, 2-methylimidazole, urate oxidase (UOx), uric acid (UA), ascorbic acid, dopamine, L-cysteine, creatinine, cholesterol, adrenaline, glucose, sucrose, mannose and nicotinamide adenine dinucleotide ($NADH^+$) were brought from Shanghai Aladdin Biochemical Technol. Co., Ltd., China. Hollow gold nanocage (citric acid-stabilized AuNC, ~80 nm in diameter, 0.1 mg mL^{-1}) was purchased from Beijing Zhongke Leiming Daojin Technol. Co., Ltd., China. Rodamine B (RhB), $FeSO_4 \cdot 7H_2O$, NaCl, KCl. ethanol and methanol were obtained from Shanghai Sinopharm Chemical Reagent Co., Ltd, China. All chemicals can be used as received without any purification. Doubly distilled water (DDW) and phosphate buffer saline (PBS) were utilized in experiments. The Affiliated Hospital of Qingdao University, China, provided fresh human serum and urine fluids as practical samples for UA detection experiments.

Compliance with Ethical Standards: All the experiments were performed in compliance with the relevant laws and institutional guidelines, and were approved by the institutional committees.

2.2. Instruments

Transmission Electron Microscopy (TEM) images and Energy Dispersive X-ray Spectrometer (EDX) data were recorded with a JEM-2100 TEM instrument (JEOL, Japan) at an acceleration voltage of 120 kV. UV-vis absorption spectra were measured with a UV–2700 (Shimadzu, Japan) spectrometer. Fluorescence (FL) excitation and emission spectra were recorded on a FL–7000 (Hitachi, Japan) spectrometer. The fluorescence lifetime study was performed using an Edinburgh FL nF900 mode single-photon counting system equipped with a Hydrogen lamp as the excitation resource. Fourier Transform Infrared (FT-IR) spectroscopy was measured by using an iS50 FT–IR (Thermo Nicolet, USA) spectrometer with KBr window in the transmission mode. Powder X-ray

diffraction (XRD) patterns were recorded with a D5005 X-ray powder diffractometer (Siemens, Germany) with graphite monochromatized Cu K_α radiation. Upon excitation with a UV lamp at 365 nm, the visual FL colors of aqueous samples were recorded with a smartphone. Square wave voltammetry (SWV) and cyclic voltammetry (CV) curves were measured by using a CHI-660E electrochemical workstation (Chenhua, China). Electrochemical impedance spectra (EIS) curves were measured through using PMC2000 electrochemical workstation (Princeton Applied Research, USA). A traditional three-electrode system was equipped for electrochemical curve measurements by using the bare glassy carbon electrode (GCE) with surface modification of different substances as the working electrode, Ag/AgCl as the reference electrode and platinum wire as the counter electrode. Each experimental result was expressed as the average of three repetitive measurements of FL spectra and electrochemical signal curves.

2.3. Preparation of UOx@MOF(AuNC) hybrid

Under stirring, 160 mg of 2-methylimidazole was dissolved in 10 mL of methanol to prepare a clear solution, followed by the dropwise addition of 1 mL AuNC aqueous suspension (0.1 mg mL^{-1}). In the resultant mixed solution, aqueous solution of $Zn(NO_3)_2 \cdot 6H_2O$ (60 mg, dissolved in 5 mL of DDW) was slowly dropped to perform stirring reaction for 15 min. Afterwards, the solution of UOx (20 mg, dissolved in 5 mL of methanol) was dropwise added to promote a further stirring reaction for 15 min. Then, the reaction solution was incubated for 12 h at 4 ℃ in a refrigerator. After incubation, the reaction solution was purified through centrifugation for 10 min at 5000 rpm, repeated washing with ethanol and DDW, and freeze-drying treatment to achieve pure and dried product of UOx@MOF(AuNC) hybrid. In the absence of AuNC and UOx, other products of MOF, MOF(AuNC) and UOx@MOF can be obtained experimentally according to the above preparation and post-treatment procedures.

2.4. Construction of UOx@MOF(AuNC) hybrid-based FL probe

Aqueous solution of $FeSO_4 \cdot 7H_2O$ was dropwise added into the aqueous suspension of UOx@MOF(AuNC) hybrid under stirring, followed by the dropwise addition of RhB to prepare a homogeneous mixture solution. The concentrations of hybrid, Fe^{2+} and RhB were fixed to be 1 mg mL^{-1}, 0.01 M and 0.1 mg mL^{-1}, respectively. In the mixture solution, UA was added to initiate tandem catalysis reactions, which finally resulted in the FL quenching responses of RhB. With the increase of existing UA concentration ([UA]) from 0 to 300 μM, FL emission spectra of mixture solution were measured under excitation at 470 nm. Relative FL intensities were calculated based on "$\Delta\mathbf{F} = \mathbf{F}_0 - \mathbf{F}$", where $\mathbf{F}_0$ and $\mathbf{F}$ stand for the emission peak intensities of FL spectra measured before and after the addition of UA. The relationship between $\Delta\mathbf{F}$ and [UA] was linearly plotted to construct a novel FL probe of UA.

2.5. Construction of UOx@MOF(AuNC) hybrid-based electrochemical sensor

A new GCE was polished with 0.3 μm and 0.05 μm alumina and was washed with DDW under sonication, followed by drying with N_2 flow. Then, 5 μL of Nafion was dropped onto the surface of clean GCE, followed by drop-casting the aqueous suspension of UOx@MOF(AuNC) hybrid (10 μL, 1 mg mL^{-1}). After rinsing treatment of GCE surface with PBS (1 mM, pH 7.4) and then natural drying in the dark place at room temperature, UOx@MOF(AuNC)/GCE was prepared and immersed in PBS as electrolyte solution. GCE surface was modified with MOF and MOF(AuNC) to form MOF/GCE and MOF(AuNC)/GCE. The CV, EIS and SWV curves of GCE with surface

modifications of different substances were measured by CHI-660E electrochemical workstation. The bare GCE and surface-modified GCE as working electrodes immersed in PBS containing 0.1 M of KCl and 5 mM of $Fe(CN)_6^{3-/4-}$ as an electrochemical signal probe. After the addition of UA (0–55 μM), SWV curves of UOx@MOF(AuNC)/GCE were measured and the redox current peak intensities of UA ($\mathbf{I}_{UA}$) were linearly plotted with the existing concentration of UA [UA]. In terms of the well-plotted linear relationship between $\mathbf{I}_{UA}$ and [UA], a facile electrochemical sensor was constructed through the novel sensing platform of UOx@MOF(AuNC)/GCE and enabled specific determination of UA.

2.6. Selectivity detection experiments of the dual-channel biosensing platform

The potential components such as Na^+, K^+, Cl^-, ascorbic acid, dopamine, L-cysteine, creatinine, cholesterol, adrenaline, glucose, sucrose, mannose and $NADH^+$, may coexist with UA in practical biological fluid samples including fresh human serum and urine. These components can serve as the interferents to potentially impact on the detection of UA. To test detection performances of the UOx@MOF(AuNC) hybrid as the dual-channel biosensing platform, selectivity experiments were carried out as below. As for the FL probe of UA, each interferent (0.5 mM), UA (50 μM) or "all interferents (6.5 mM) *plus* UA (50 μM)" was respectively added into the mixture solution that contains the hybrid, Fe^{2+} and RhB to prepare a series of homogeneous mixture solutions under stirring. FL emission spectra of the resultant mixture solutions were measured and the relative FL intensities ($\mathbf{F}_0 - \mathbf{F}$, $\mathbf{F}_0$ and $\mathbf{F}$ stand for FL emission peak intensities before and after the respective additions of each interferent, UA and "all interferents *plus* UA") were compared, so as to evaluate selective FL responses of the probe toward UA. As for the electrochemical sensor of UA, SWV curves of UOx@MOF(AuNC)/GCE were measured in the presence of each interferent (0.2 mM), UA (20 μM) and "all interferents (2.6 mM) *plus* UA (20 μM)", respectively. The UA-redox peak current (**I**) intensities peaked at 0.3 V were calculated. "**I**" values from the corresponding SWV curve measurements after respective additions of each interferent, UA and "all interferents *plus* UA" were compared to evaluate selective electrochemical signal responses toward UA.

2.7. Detection experiments of UA in biological samples

In detail, fresh human serum and urine fluids as practical samples were used for UA detection in experiments. Practical samples were 100-fold diluted with PBS (1 mM, pH7.4) to prepare sample solutions. With regard to the FL probe, each sample solution was added into the mixture solution containing the hybrid, Fe^{2+} and RhB, followed by the addition of UA to form a series of sample- probe solutions without and with the addition of UA. The final coexisting concentration of UA was fixed to be 10, 50, 100 or 250 μM. By measuring the FL emission spectra of sample-probe solutions, the concentrations of UA in samples can be calculated by the plotted linear relationship between $\Delta\mathbf{F}$ and [UA]. As for the electrochemical sensor, SWV curves of UOx@MOF(AuNC)/ GCE were measured from each sample solution without and with the addition of UA. The final coexisting concentration of UA was fixed to be 10, 20 or 50 μM. According to the plotted linear relationship between $\mathbf{I}_{UA}$ and [UA], the corresponding concentrations of UA in different samples can be calculated and compared with the spiked ones.

Table S1

Brief summaries of different sensing platforms and their performances for the detection of UA.

Sensing platform	Transducer	Linear range /μM	LOD /μM	References
Au@NAC-MWCNTs	DPV	0.1–300	0.04	[1]
Au-Ag NPs/GO/TH	SWV	1–100	0.3	[2]
$Ni(OH)_2$-solar graphene	DPV	2–15	0.46	[3]
Graphene flowers	DPV	3.98–371.4	3.98	[4]
Graphene/PANI/Au	DPV	140–2900	47	[5]
AuNPs@MoS_2	DPV	10–7000	10	[6]
MoS_2/PEDOT	DPV	2–25	0.95	[7]
ERGO	DPV	0.5–60	0.5	[8]
Graphene/SnO_2	DPV	3–21	3	[9]
Pd/CNF-CPE	DPV	2–200	0.7	[10]
CoTe/graphite paste	DPV	10–120	0.895	[11]
Fe@NCDs	Colorimetry	2–150	0.64	[12]
Ni GLAD	Colorimetry	15–500	3.3	[13]
Uricase/Th-MOF	Colorimetry	4–70	1.15	[14]
Silicon nanoparticles	Fluorescence	10–800	0.75	[15]
PVP-AuNPs/CS-AuNCs	Fluorescence	1–100	0.3	[16]
Cu(II)/Cu_2O/N-GQDs	CL	0.16–4	0.041	[17]
Ag-CDs nanocomposites	SERS	1–500	–	[18]
UOx@MOF(AuNC)	SWV	0.05–55	0.015	This work
UOx@MOF(AuNC)	Fluorescence	0.1–10, 10–300	0.02	This work

Abbreviation: Au@NAC-MWCNTs, multiwall carbon nanotubes functionalized with N-acetyl-l-cysteine stabilized gold clusters; Au-Ag NPs/GO/TH, graphene oxide-thionine complex on Au-Ag bimetallic nanoparticles; PANI, polyaniline; AuNPs, gold nanoparticles; PEDOT, 3,4-ethylenedioxythiophene; ERGO, electrochemically reduced graphene oxide; CNF-CPE, carbon nanofibers/carbon paste electrode; Fe@NCDs, carbon quantum dots co-doped with iron and nitrogen; Ni GLAD, helically structured Ni thin films deposited by glancing angle deposition; PVP- AuNPs, poly(vinylpyrrolidone)-protected gold nanoparticles; CS-AuNCs, chondroitin sulfate-stabilized gold nanoclusters; N-GQDs, nitrogen atom-doped graphene quantum dots; CL, chemiluminscence; Ag-CDs, silver nano particles-carbon dots; SERS, surface-enhanced Raman scattering.

Table S2

Practical detection of UA in real biological samples through using the UOx@MOF(AuNC) hybrid-based FL probe.

Sample	Spiked UA /μM	Detected UA /μM Average ± standard deviation (SD, n=3)	RSD /% (SD/average) ×100%	Recovery /%
Serum	0	Not detected	–	–
	10	9.57 ± 0.21	2.19	95.70
	50	47.65 ± 1.53	3.21	95.30
	100	104.20 ± 3.59	3.44	104.20
	250	261.77 ± 10.12	3.87	104.71
Urine	0	13.15 ± 0.62	4.71	–
	10	24.10 ± 1.03	4.27	104.10
	50	61.37 ± 2.12	3.45	97.18
	100	115.80 ± 2.05	1.77	102.34
	250	259.46 ± 8.39	3.23	98.60

Table S3

Practical detection of UA in real biological samples through using the UOx@MOF(AuNC)/GCE platform-based electrochemical sensor.

Sample [a]	Spiked UA /μM	Detected UA /μM Average ± SD (n=3)	RSD /% (SD/average) ×100%	Recovery /%
Serum	0	Not detected	–	–
	10	9.62 ± 0.45	4.67	96.20
	20	20.27 ± 0.76	3.75	101.35
	50	48.58 ± 2.14	4.40	97.16
Urine	0	11.25 ± 0.24	2.13	–
	10	20.76 ± 0.33	1.59	97.69
	20	30.81 ± 0.89	2.89	98.59
	50	62.10 ± 1.31	2.11	101.39

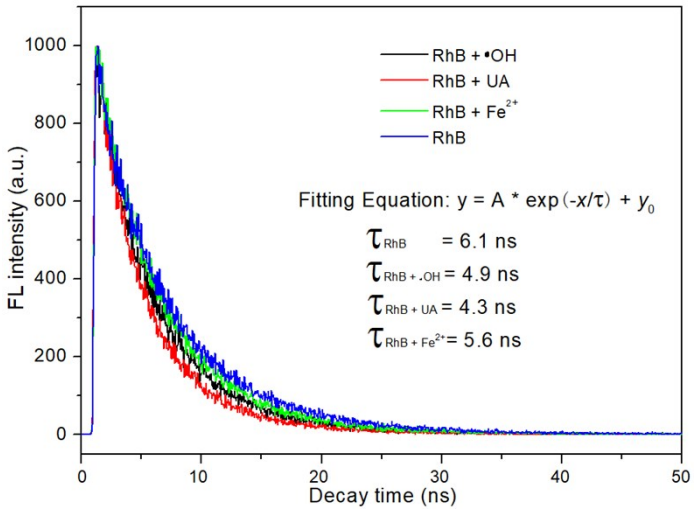

Fig. S1. FL decay curves of sole RhB and RhB with the respective additions of •OH, UA and Fe^{2+}. FL lifetimes were measured through a single exponential curve fitting for RhB and RhB additives. Emission wavelength (λ_{em}) was monitored at the first exitonic peak wavelength of RhB (600 nM).

As shown in Scheme 1, to design the hybrid-based FL biosensing platform, a tandem catalysis system was constructed in the aqueous solution that contains the hybrid, Fe^{2+} and RhB. After the addition of UA, UA was enzymatically oxidized by the hybrid to generate H_2O_2, and then H_2O_2 reacted with Fe^{2+} to generate •OH hydroxyl radical through the Fenton oxidization. The following reaction of •OH with RhB induced the oxidization, decolorization and then FL quenching of RhB [19–23]. As for FL quenching of RhB, the potential mechanism can be explained as below [19].

$H_2O_2 + Fe^{2+} \rightarrow Fe^{3+} + •OH + OH^-$

$H_2O_2 + Fe^{3+} \rightarrow Fe^{2+} + •HO_2 + H^+$

$•OH + H_2O_2 \rightarrow •HO_2 + H_2O$

$•OH + Fe^{2+} \rightarrow Fe^{3+} + OH^-$

$Fe^{3+} + •HO_2 \rightarrow Fe^{2+} + O_2 + H^+$

$Fe^{2+} + •HO_2 + H^+ \rightarrow Fe^{3+} + H_2O_2$

$•HO_2 + •HO_2 \rightarrow H_2O_2 + O_2$

RhB + •OH → Decolorized RhB

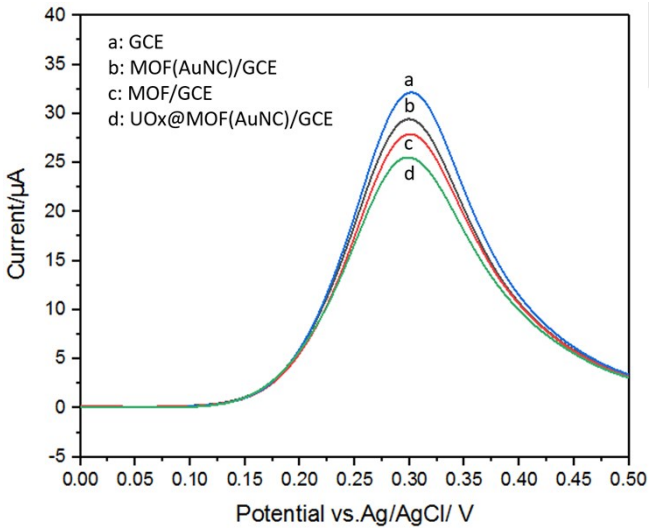

Fig. S2. SWV curves of bare GCE and GCE modified with MOF, MOF(AuNC) or UOx@MOF (AuNC) hybrid, respectively. Bare GCE and modified GCE (working electrodes) as the sensing platforms were respectively immersed into PBS (1 mM, pH 7.4) with the addition of UA at the identical coexisting UA concentration (1 μM).

References

[1] Z. Wang, H. Guo, R. Gui, H. Jin, J. Xia and F. Zhang, *Sens. Actuators B*, 2018, **255**, 2069–2077.
[2] X. Gao, R. Gui, K. Q. Xu, H. Guo, H. Jin and Z. Wang, *New J. Chem.*, 2018, **42**, 14796–14804.
[3] T. E. M. Nancy and V. A. Kumary, *Electrochim. Acta*, 2014, **133**, 233–240.
[4] J. Du, R. Yue, F. Ren, Z. Yao, F. Jiang, P. Yang and Y. Du, *Biosens. Bioelectron.*, 2014, **53**, 220–224.
[5] L. Shi, Z. Wang, G. Gou, X. Chen, G. Yang and W. Liu, *Int. J. Electrochem. Sci.*, 2017, **12**, 2540–2551.
[6] H. Sun, J. Chao, X. Zuo, S. Su, X. Liu, L. Yuwen, C. Fan and L. Wang, *RSC Adv.*, 2014, **4**, 27625–27629.
[7] Y. Li, H. Lin, H. Peng, R. Qi and C. Luo, *Microchim. Acta*, 2016, **183**, 2517–2523.
[8] L. Yang, D. Liu, J. Huang and T. You, *Sens. Actuators B*, 2014, **193**, 166–172.
[9] Y. L. Xie, J. Yuan, H. L. Ye, P. Song and S. Q. Hu, *J. Electroanal. Chem.*, 2015, **749**, 26–30.
[10] J. Huang, Y. Liu, H. Hou and T. You, *Biosens. Bioelectron.*, 2008, **24**, 632–637.
[11] S. Pradhan, R. Das, S. Biswas, D. K. Das, R. Bhar, R. Bandyopadhyay and P. Pramanik, *Electrochim. Acta*, 2017, **238**, 185–193.
[12] C. Liang, Y. Lan, Z. Sun, L. Zhou, Y. Li, X. Liang and X. Qin, *Microchim. Acta*, 2020, **187**, 405.
[13] A. Tripathi, K. D. Harris and A. L. Elias, *ACS Omega*, 2020, **5**, 9123−9130.
[14] A. Badoei-dalfard, N. Sohrabi, Z. Karami and G. Sargazi, *Biosens. Bioelectron.*, 2019, **141**, 111420.
[15] C. Wu, L. Zhu, Q. Lu, H. Li, Y. Zhang and S. Yao, *Microchim. Acta*, 2019, **186**, 754.
[16] Y. Liu, H. Li, B. Guo, L. Wei, B. Chen and Y. Zhang, *Biosens. Bioelectron.*, 2017, **91**, 734−740.
[17] B. Shi, Y. Su, Y. Duan, S. Chen and W. Zuo, *Microchim. Acta*, 2019, **186**, 397.
[18] A. Wang, C. Guan, G. Shan, Y. Chen, C. Wang and Y. Liu, *Microchim. Acta*, 2019, **186**, 644.
[19] Q. Chi, *Guangzhou Chem. Ind.*, 2017, **45**, 85–87.
[20] F. Jiang, G. Cao, Y. Zhuang and Z. Wu, *React. Kinet. Mech. Cat.*, 2020, **130**, 1093–1108.
[21] L. Kai, K. Yue and X. Ma, *Bull. Sci. Technol.*, 2008, **24**, 183–187.
[22] Q. Wang, H. Wei, Z. Zhang, E. Wang and S. Dong, *Trend Anal. Chem.*, 2018, **105**, 218–224.
[23] T. Wang, X. Hu, X. Zhang, H. Cao, Y. Huang and P. Feng, *Anal. Methods*, 2019, **11**, 415–420.